



Gait-based Person Identification using Multiple Inertial Sensors

Osama Adel¹^a, Yousef Nafea¹, Ahmed Hesham¹ and Walid Gomaa^{1,2}^b

¹Cyber-Physical Systems Lab, Department of Computer Science and Engineering,
Egypt-Japan University of Science and Technology, Borg El-Arab, Alexandria, Egypt

²Faculty of Engineering Alexandria University, Alexandria, Egypt

Keywords: Gait, Person Identification, Multi-sensory, Inertial Sensors, Human-centered Computing.

Abstract: Inertial sensors such as accelerometers and gyroscopes have gained popularity in recent years for their use in human activity recognition. However, little work has been done on using these sensors for gait-based person identification. Gait-based person identification turns out to be important in applications such as where different people share the same wearable device and it is desirable to identify who is using the device at a given time while walking. In this research, we present the first multi-sensory gait-based person identification dataset EJUST-GINR-1 and present our work on gait-based person identification using multi-sensory data, by mounting 8 wearable inertial sensory devices on different body locations and use this data to identify the person using it. Two of these sensors are smart watches worn on both wrists. We explore the correlation between each body location and the identification accuracy, as well as exploring the effect of fusing pairs of sensory units in different locations, on the final classification performance.

1 INTRODUCTION

Inertial sensors such as accelerometers and gyroscopes have gained a renowned reputation in recent years for their use in human activity recognition (HAR). These sensors can capture the motion dynamics of different parts of the human body, and stream this data to a processing unit for further analysis. By analyzing the streamed data (either in real-time or offline), we can classify the motion done by a human as one of different activities, which proved to be helpful in a plethora of applications specifically, in the sports and healthcare fields (Patel et al., 2012).


However, inertial sensors haven't received enough attention in *Gait-based Person Identification*. Gait-based Person Identification using inertial sensors is concerned with the problem of identifying a person from a predefined set of people using one or more inertial measurement units mounted on the body while walking. It's different from *person authentication or verification* in the sense that the later addresses the problem of identifying if a certain person is proper one wearing the (embedded) inertial sensors or not. Since gait patterns are unique for each individual, given the inertial sensors readings of an individual's


gait patterns, that individual should be correctly and uniquely identified (Tao et al., 2018).

Machine learning algorithms (including deep learning) have been widely used in human activity recognition (Lara and Labrador, 2013) and should show good results in person identification as well. Despite the wide use of deep learning techniques, some traditional machine learning still achieves comparable performance in activity recognition especially, with much less computational demands, when the amount of data available is small (Abdu-Aguye and Gomaa, 2019).

Person identification is of interest, for example, when a wearable device is shared among a group of people, and it is desirable to distinguish the person who is wearing or using the device. It can be especially helpful in sports teams, where activity tracking devices are shared among different members and an automatic detection of the person wearing the device at a given moment is desired to automatically stream data to her profile. Hence, it has become really important to identify the person who uses the device at that moment.

In this work, we focus on person identification using multiple inertial sensory devices mounted on different locations on human body. We try to answer two questions:

^a <https://orcid.org/0000-0003-3471-5787>

^b <https://orcid.org/0000-0002-8518-8908>

1. *Which body locations/placements for an inertial sensory device, are the most indicative of a person identity assuming the action of 'walking'?*
2. *What is the impact of fusing pairs of those sensory devices on the final classification performance?*

To answer these two questions, we constructed a new dataset, EJUST-GINR-1¹, of 20 persons using 8 inertial wearable devices mounted on 8 fixed locations on each person's body. We used three different machine learning models for person identification: Random Forest Classifier, Support Vector Machine (SVM), and Convolutional Neural Network (CNN). Each was trained in two different ways: on 8 single sensory device data in order to investigate the impact of differing the location of the sensor on the classification performance, and on a fused pairs of devices, to explore the effect of sensor fusion on person identification.

The rest of this paper is organized as follows. Section 1 is an introduction. We present the related work in Section 2. Section 3 is a detailed demonstration of the data collection and cleaning process. In Section 4 we demonstrate our data pre-processing and feature selection procedures, in Section 5 we present our experiments including our machine learning models and the metrics used for evaluating them. Then we present our results in Section 6, and finally Section 7 is our conclusion.

2 RELATED WORK

(Kwapisz et al., 2010) collected 3-axis accelerometer data from different Android smartphones inserted in the pockets of 36 users while they perform different activities including walking, then they divide the collected data into 10-second examples, do feature extraction using six basic statistical features on each axis ending up with 43-D feature vector, and feed this feature vector to two classifiers: a decision tree and a neural network. Their work showed that person identification was possible with accuracy up to 90% on walking data using neural networks.

(Ngo et al., 2014) presented the largest inertial sensors gait database for personal authentication. The authors collected data from 744 subjects with ages ranging from 2 to 78 years, an almost balanced male-to-female ratio - using 4 sensors, 3 IMU sensors on the left, right and center of the waist, in addition to a smartphone on center of the waist. Two 6-D 1-min sequences were recorded for each subject during walking a designed path on his normal speed. The path

¹Dataset and code are available upon request.

has a flat and a slope ground, and one of the two sequences was recorded on the slope ground. Then, for authentication, a template (or gallery) was created for the owner's data and to decide if a new sequence of data (a probe pattern) belonged to the same person, a distance function was used to calculate the difference between the gallery and the probe pattern and if the difference was below a certain threshold, the user was considered the legitimate one.

(Cola et al., 2016) demonstrated a light-weight method for gait-based user authentication using data collected from an accelerometer wrist sensor. A profile of a user is created on first-time use, then anomalies in acceleration data could detect a stranger using the device. Evaluated successfully with 15 volunteers with Equal Error Rate (EER) of 2.9%, they showed that person authentication using wrist-worn device can achieve high accuracy.

(Mondol et al., 2017) used a wrist-worn accelerometer and gyroscope sensors embedded in a smartwatch while doing a gesture in the air to authenticate the user of the smartwatch. The purpose of this work was to provide an alternative method for authenticating the true owner of a smartwatch or a smartphone using a unique gesture. Each participant in this study performed a unique gesture in the air, such as performing a signature, a number of times to create a template for his unique gesture. Then, a new user would try to replicate his signature, and the Dynamic Time Warping (DTW) was used to measure the deviation between the two data gestures. The signature is accepted only if the deviation is below a predefined threshold.

As far as we know, this is the first work done on gait-based person identification using multiple inertial sensory devices mounted on different upper and lower body parts, and the first to study the impact of the location and fusion of sensory devices at different locations on the final identification performance, as well as the first to provide a dataset collected for multi-sensory gait-based person identification with sufficient number of samples and subjects - publicly available for the research community.

3 DATASET CONSTRUCTION

We recorded walking activity data from inertial sensory devices mounted on 8 locations (Figure 1) on 20 subjects, to use these data to identify the person wearing the sensory devices.

All the participants in data collection of EJUST-GINR-1 dataset are students (undergraduate and post-graduate) at our university, with ages ranging from

19 – 26, weights from 56 – 130 kg, heights from 146 – 187 cm, and a 1:1 male-to-female ratio. Table 1 shows an overview of the subjects in our dataset.

Table 1: An overview of the subjects in EJUS-TGINR-1.

Features	Min	Max	Mean	Stdv
Age	19	26	21.15	2.30
Height (cm)	146	187	169.4	10.15
Weight (kg)	56	130	76.37	16.46
Lap time (min)	4	4.3	4.2	0.025

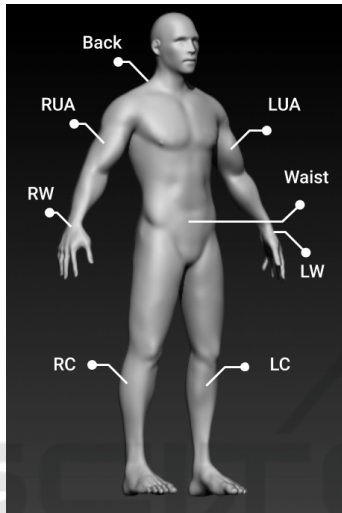


Figure 1: Locations of sensory devices on a subject’s body.



Figure 2: Data capture system. Two Apple watches on the left, an iPhone 7 and 6 MMR devices in the middle. Three velcro sleeves on the right.

We used two types of sensory devices in our data capture system: Apple Watches Series 1 and Mbi-ent-Lab MetaMotionR (MMR) sensory devices. Two Apple watches were worn on the right and on the left wrists (RW and LW) of the subjects, and 6 MMR sensory devices were mounted on the following 6 locations on each subject’s body: the right upper arm (RUA), the left upper arm (LUA), the back, the waist, the left and right calfs (LC and RC). These locations are illustrated in Figure 1. Additionally, we have used

an iPhone 7 in the recording activity, as all MMR devices had to be connected to it during the recording session until the data recorded is transferred, and because the data collected on the Apple watches had also to be transferred to the iPhone after the end of the data recording activity. Figure 2 shows the entire data capture system described above.

Both Apple watches and MMR devices came packed with a large number of embedded sensors such as: 3-axis accelerometer, 3-axis gyroscope, 3-axis magnetometer, pressure sensor, humidity sensor and others. However, we only considered the recordings of the 3-axis accelerometer and 3-axis gyroscope from both the Apple watch and MMR devices at sampling rate of 50 Hz.

For every recording session, each subject walked a path (around our university’s HQ building) of about 330 meters long taking about 4 minutes on average. Each subject recorded 4 sessions with a total of about 16 minutes of walking activity, and since we recorded 4 laps for each of the 20 subjects, our dataset is composed of about 5 hours of walking activity data collected from 8 different sensory devices synchronously.

3.1 Data Cleaning

Figure 3 shows the first 30 seconds of the 3-axis accelerometer’s signals recorded from the sensory device on the Left Upper Arm (LUA) of two randomly selected subjects (number 13 and 14). From this figure, it is obvious that there is a period (about 600 samples or 12 seconds) in the start of each session where there is no activity done. This period of non-walking activity is problematic since it will be fed to our models as walking activity. Certainly, this will confuse our models and decrease their performance and consequently, they must be removed. This was done by manually inspecting the recording session of every sensory device for every subject then trimming the parts that showed no-activity or high levels of noise.

The final structure of our dataset is as follows: each sensory device has a separate folder containing 20 files, each representing the data collected from one subject and each subject’s file contains all 4 recording sessions appended to each other. We used the *Numpy* framework to store each subject’s data in *.npy* format, as *Numpy* is the most popular Python framework for multi-dimensional array manipulation. Each *.npy* file is a $M \times 6$ matrix, where M represents the number of entries/samples per subject while 6 corresponds to the concatenation of 3-axis accelerometer and 3-axis gyroscope columns.

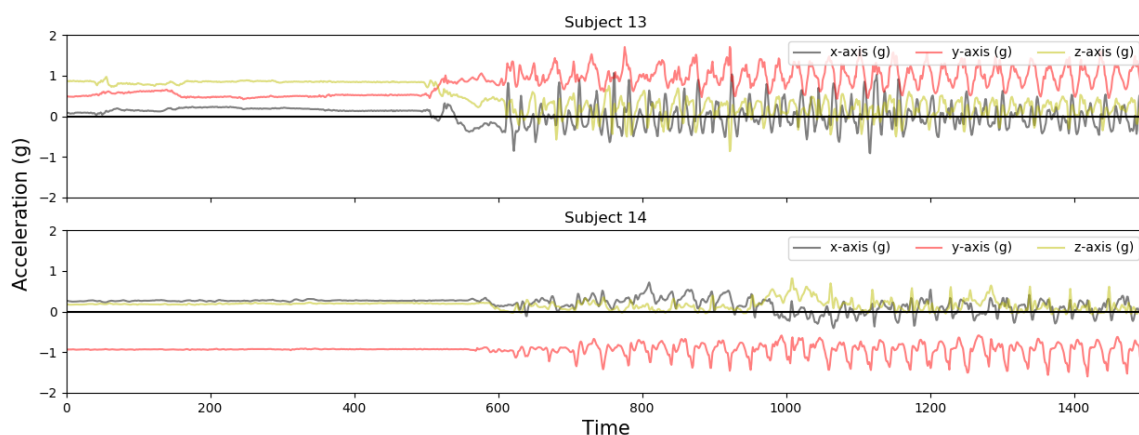


Figure 3: The first 30 seconds of two sequences of walking activities of two randomly selected subjects recorded from the Left Upper Arm (LUA) device.

4 METHODOLOGY

4.1 Data Preprocessing

We devised a preprocessing stage composed of 4 steps: data loading and labeling, segmentation, shuffling and one-hot encoding. In the data loading and labeling step, given a specific sensory device, we load all the '.npy' files for all subjects in the given device's folder, then we concatenate the corresponding labels to them. Next is the segmentation step, where we divide the loaded data into non-overlapping t -second segments. Since we use 50 Hz as the sampling rate across all devices and recording sessions, the total number of segments M resulting from segmentation of the data into t -second segments can be calculated from the following formula:

$$M = \frac{L}{50 * t} \tag{1}$$

where L is the length of samples recorded for all subjects given a single sensory device. Based on the work in (Murray et al., 1964) the average duration of one gait cycle for men with ages from 20 to 65 is about 1.03 seconds. Since our subjects are both men and women, and we use sensors on many different locations, we decided to set the duration of a single segment to be 5 seconds ($t = 5$) to make sure that each segment contains enough information for sound classification. Therefore, given that each sensory device recorded about 868511 samples (for all subjects) on average, the total number of segments for each device is $M = 868511 / (5 * 50) \approx 3474$. After that, we shuffled the data segments randomly because they were ordered ascendingly according to the labels (from 0 to 19) and randomization would help the models train

better without bias. Furthermore, some classifiers such as Convolutional Neural Networks require the labels to be in one-hot encoding format, hence, we had to convert the labels from a M -D vector to a $M \times 20$ one-hot encoded matrix, where M is the number of segments and 20 is the number of classes.

The result of the preprocessing stage is a list X of M segments (calculated from Equation 1), each segment is a 250×6 matrix, where 250 is the number of samples per 5-second segment and 6 is the number of features/columns/axes per segment - in addition to a $M \times 20$ one-hot encoded labels matrix.

4.2 Feature Extraction (FE)

Given that each segment in list X is 250×6 matrix, the dimension of the input space to our machine learning models must be in \mathbb{R}^{1500} which is huge. Moreover, each segment represents the raw data collected from the inertial sensors which are not useful on themselves. Hence, an additional step to reduce the dimensionality of the input space and to extract meaningful features is required. In this work, we use the *autocorrelation* statistical feature extractor based on the work done in (Gomaa et al., 2017).

The Auto-Correlation Function (ACF) of a sampled time-series signal x_t calculates the Pearson correlation between x_t and a shifted version of itself x_{t+h} by a lag h , assuming x_t is weakly stationary. This can give us information about the dependency of the signal to its shifted version (Shumway and Stoffer,), which can be particularly useful in periodic activities such as walking. Therefore, given different input lags, the Auto-Correlation Function can be calculated for each lag h using the following formulas:

$$acf_x(h) = \frac{\gamma_x(h)}{\gamma_x(0)} \quad (2)$$

$$\gamma_x(h) = \frac{1}{T} \sum_{t=1}^{T-h} (x_{t+h} - \bar{x})(x_t - \bar{x}) \quad (3)$$

where \bar{x} is the sample mean of the signal x and T is the length of the sampled signal x .

Assuming that our input data sample has K features/columns/axes, we can calculate the ACF over each column in the input segment over a set of different lags. The output will be a scalar for each lag that summarizes the T entries (where $T = 250$) along one column of the input segment. We calculate the ACF for each one of the K columns for N lags (starting from $N = 0$), which will result in a $K(N + 1)$ -D feature vector as follows:

$$[acf_1(0) \dots acf_K(0) \ acf_1(1) \dots acf_K(1) \dots acf_K(N)]$$

To calculate the ACF over all M segments in our input list X for a set of N lags, which would result in a $M \times K(N + 1)$ features matrix, we implemented the following algorithm (Algorithm 1):

Algorithm 1: Feature Extraction Algorithm.

```

input : List  $X$ ,  $N \in \mathbb{R}$ 
output:  $\hat{X} \in \mathbb{R}^{M \times KN}$ 
Initialize  $\hat{X}$  with zeros,  $i \leftarrow 0$ ;
foreach  $s \in X$  do
  for  $h \leftarrow 0$  to  $N$  do
    for  $k \leftarrow 0$  to  $K - 1$  do
       $\hat{X}_{i, Kh+k} = acf_k(h)$  (From Eq. 2)
    end
  end
   $i \leftarrow i + 1$ ;
end

```

5 EXPERIMENTS

We conducted two experiments: the first aims at exploring the effect of a single location/placement of an inertial sensory device on the final person identification performance, whereas the goal of the second was to investigate how fusing different pairs of inertial sensory devices worn on 8 different locations on the human body while walking (Figure 1) - affects the person identification performance.

In both experiments, we started by loading the data (individual devices in the first experiment, and pairs of devices in the second), then we pre-processed the loaded data as discussed in Section 4.1, did feature extraction as shown in Section 4.2 (choosing the

number of columns K to be 6 in the first experiment, and to 12 in the second), and the number of lags N to be 10 based on the work done in (Gomaa et al., 2017), split the features matrix and the corresponding labels into training and test sets (80 – 20% train-test split), trained 3 classification models: a Random Forest (criterion for a split is the gini-index, number of grown trees = 100, minimum number of samples to split a node = 2 and using bootstrapping), a Support Vector Machine (linear kernel, hinge as the loss function, regularization parameter $C = 1$, maximum number of iterations = 1000 and One-Vs-The-Rest as the multi-class SVM implementation) and a Convolutional Neural Network (as shown in Figure 5) - using the training set, evaluated the models performance using two metrics: accuracy and f1-measure - on the test set and eventually stored the evaluation metrics results for each model for further analysis.

The up-mentioned pipeline (illustrated in Figure 4) was repeated for every sensory device (in the first experiment) and each 28 possible pairs of sensors (in the second experiment) saving the results separately. Moreover, to ensure that our results are consistent, we ran the previous steps 15 times, each on a different and random train-test split (again, 80 – 20% train-test split), then taking the average of the results over the 15 trials.

6 RESULTS AND DISCUSSION

In order to interpret the results obtained in both experiments, a *Fusion Matrix* has been constructed, where every entry $f_{i,j}$ represents the score achieved by fusing device i with device j while the entries at the diagonal where $i = j$ represent the scores of individual devices i obtained from the first experiment. The Fusion Matrix is a symmetric matrix since the fusion of device i with device j is the same in reverse. For each classifier of the 3 we used, two Fusion Matrices have been constructed, one for the accuracy and another for the F1-measure.

By examining the diagonal of the 6 Fusion Matrices shown in Figure 6 and 7, it is clear that the sensory devices mounted on either the left calf (LC) or right calf (RC) achieved the highest accuracy and F1-measure. Using CNN, the highest accuracy and F1-measure were achieved on the LC with 98.6% and 0.99, whereas the accuracy and F1-measure achieved using CNN on the RC were 97.3% and 0.97, respectively. On the other hand, SVM achieved 96.8% accuracy on LC, 96.4% accuracy on RC, 0.97 F1-measure on LC and 0.96 F1-measure on RC. Our Random Forest model, despite being simple, achieved 95% ac-

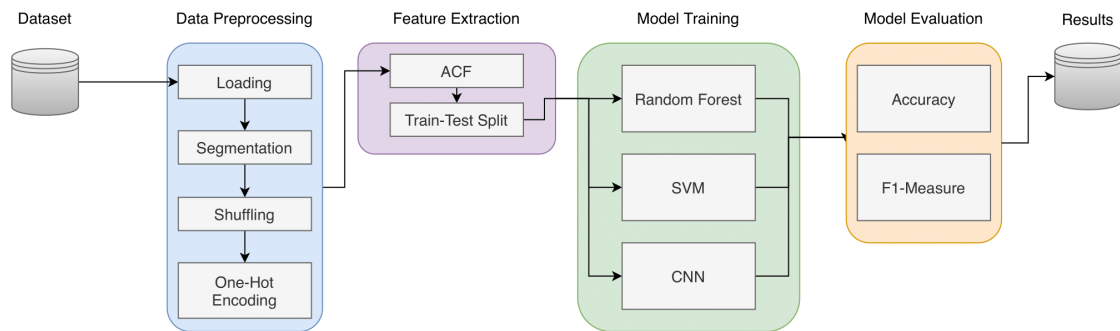


Figure 4: Stages of our experiments pipeline.

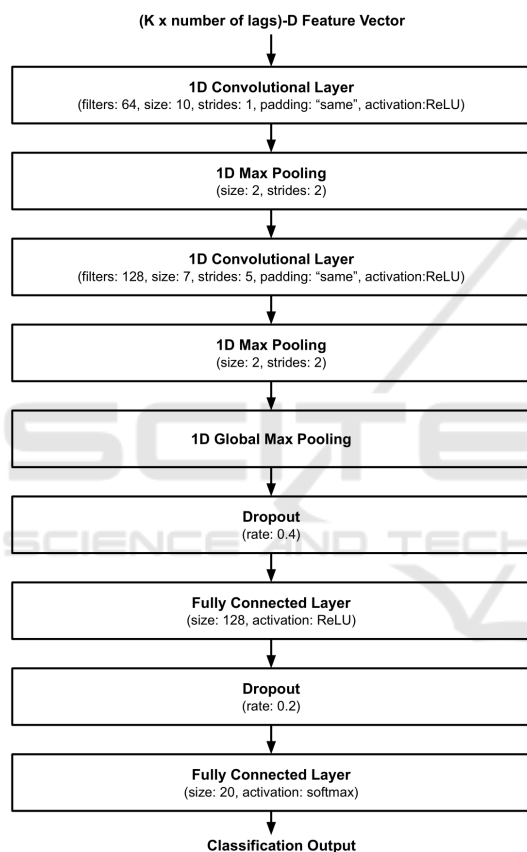


Figure 5: CNN architecture.

accuracy on LC and 95.5% on RC, in addition to 0.95 F1-measure on both LC and RC. Likewise, the device mounted on the waist was able to score 96.9% accuracy and 0.97 F1-measure using CNN. At about 94% accuracy, SVM was the second best before Random Forest, which achieved 92.7% accuracy on the same device.

On the other hand, the sensory devices worn on both the left wrist (LW) and right wrist (RW) showed the worst results. Again, CNN performed better than SVM and Random Forest, achieving 82.8%

accuracy for the LW and 82.3% for the RW. Similarly, it achieved 0.83 and 0.82 F1-measures on the LW and RW, respectively. The performance of the other two models was close, with an edge to SVM at about 77% and 76.4% accuracy for the LW and RW whereas Random Forest achieved 75.6% and 74% accuracy, respectively. The F1-measure of both models achieved similar results.

Surprisingly, the identification accuracy achieved using the data collected from the sensory device on the back was about 96.8% with CNN, 94% with SVM and 93% with Random Forest - despite being the furthest from the lower body sensory devices. The same goes with F1-measure with 0.97, 0.94 and 0.93, respectively. This is the third best accuracy achieved over all the devices, which means that the gait pattern was clearly captured by this device, and that this location is the best in the upper body for person identification.

The classification accuracy of the fusion of two sensory devices can be seen in the off-diagonal entries in the 3 Fusion Matrices shown in Figure 6. As we can see, in all cases the fusion of two sensory devices results in an overall accuracy higher than that of the single lower-accuracy device. For example, The Random Forest Classifier accuracy on data collected from the device on the RW individually is about 74%, however, when combined with any other device, the accuracy drastically increases, up to 96% when combined with either the RC or LC. The same is true with SVM, as the accuracy jumps from 76% for RW up to 98% when combined with LC, which is substantially higher than the average of their combined accuracy (86.5%).

On the other side, this means that combining one of the devices with very high individual accuracy with another very low individual accuracy can result in a degradation of the classification power gained from the high-accuracy device. Specifically, fusing one of the devices mounted on the lower body with another device worn on the upper body results, in most cases,

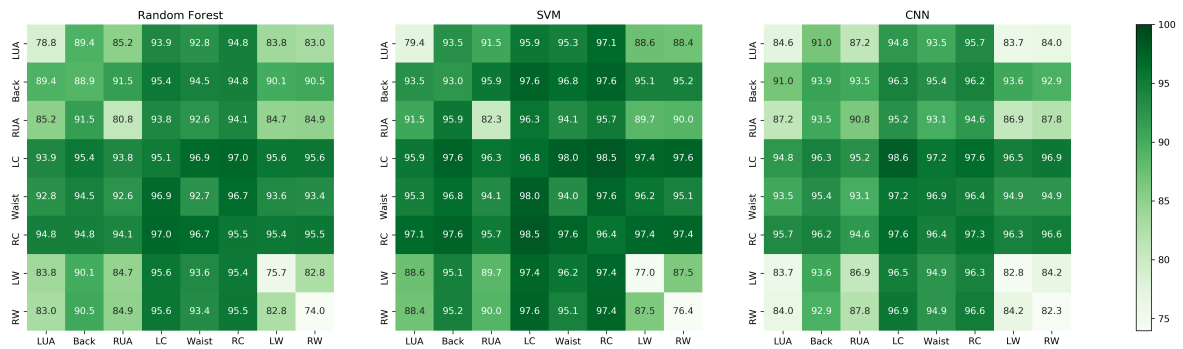


Figure 6: Accuracy Fusion Matrix for Random Forest, SVM and CNN.

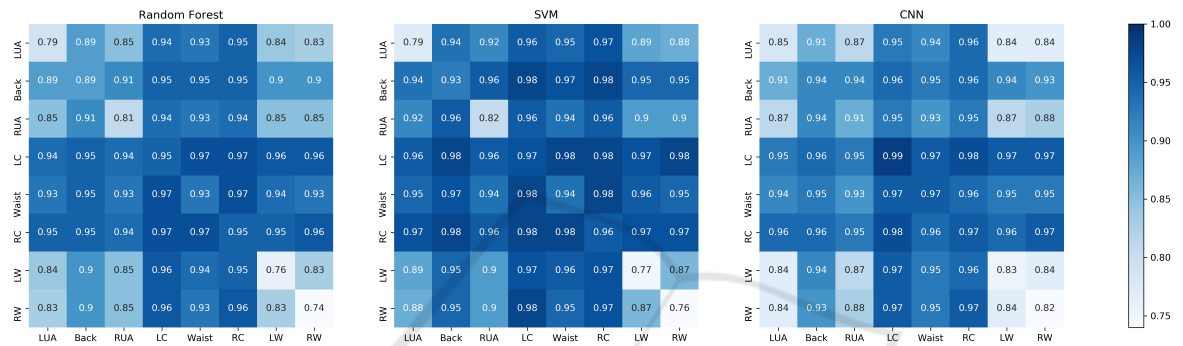


Figure 7: F1-Measure Fusion Matrix for Random Forest, SVM and CNN.

in a lower accuracy than that of the individual lower body device. For example, the device worn on the LC achieves 95%, 97% and 99% accuracy with Random Forest, SVM and CNN, respectively. When combining this device with RUA or LUA devices, the accuracy drops to 94% with Random Forest Classifier, 96% with SVM and 95% with CNN.

Therefore, the best fusion of devices will be between two lower-body devices especially, LC and RC, since they produce up to 97% accuracy even with simple classifiers such as Random Forest, and up to 98% accuracy with SVM and CNN. However, fusing the data from the device on the back with data from either RC or LC also results in an accuracy up to 98% with SVM. Besides, fusing either RC or LC devices with RW or LW devices appears to achieve higher accuracy than fusing RC or LC with RUA or LUA, up to 98% (LC + RW under SVM).

From the previous results, it can be deduced that the devices mounted on the lower part of the body achieve better classification performance in general and are more indicative of the person wearing them while walking - than the devices mounted on the upper body parts. This can be attributed to the fact that people have more freedom to move their hands and arms while walking in different ways than they have with their legs and waist while walking, which

may induce noise in the inertial sensors readings from these locations. Possibly, being able to extract discriminative features from such noisy data might help increase the accuracy of models trained on such data. However, recording data from an inertial sensory device placed on the back (of the neck) achieves second-best performance after sensory devices placed on the lower body. One explanation might be that the gait patterns were transmitted almost intact through the backbone up to this location.

Generally, SVM achieves better results compared to CNN in the fusion of pairs of devices. This may have stemmed from the fact that we merge the columns in the input data in order to merge two devices. However, the architecture of the CNN was designed to accommodate only 6 columns. This is a result of using the Global Max Pooling layer which takes the maximum value out of each feature map and returns a vector with size equal to the number of feature maps. Since the architecture of the network is the same, doing the same convolution operations on a larger input feature space results in a larger feature maps at the last layer, and taking the maximum directly may have resulted in a great loss of information and as a result, loss in classification power as well. On the other hand, the SVM we used is with a linear kernel thus, it is a linear classifier, which benefits from

the increase in the number of features as it adds more separability power to it. The F1-measure closely follows the accuracy in almost all cases. This means that our models correctly classify each person correctly without any bias towards a single class/individual.

7 CONCLUSIONS AND FUTURE WORK

In this work, a novel multi-sensory dataset was presented with detailed demonstration of all the steps taken for its construction. Additionally, three different machine learning algorithms were used to evaluate the new dataset, and to explore the correlation between the on-body location of sensory device - with the model accuracy as well as, the effect of fusing pairs of sensory data from different body locations on the resultant predictive performance. It turns out that, the sensory devices mounted on the lower body achieved better performance (up to 99% accuracy) than sensors worn on the wrist or on the upper arm. However, the sensory device mounted on the back achieved a comparable accuracy despite being far away from the gait.

It was also shown that fusing sensory data from two different locations help increasing the classification accuracy above the low-accuracy single location, and increases the accuracy significantly if fused with a device mounted on one of the three locations in the lower body (up to 98%).

Finally, the data collected in this work included only walking activity. However, in the future, we would like to explore more activities such as: brushing teeth, climbing stairs, jogging, etc., and investigate if they can constitute bio-metric features for different people. We would also like to study the impact of sensory devices' location on the identification performance for each activity.

ACKNOWLEDGEMENTS

This work is funded by the Information Technology Industry Development Agency (ITIDA), Information Technology Academia Collaboration (ITAC) Program, Egypt – Grant Number (PRP2019.R26.1 - A Robust Wearable Activity Recognition System based on IMU Signals).

REFERENCES

- Abdu-Aguye, M. G. and Gomaa, W. (2019). Competitive Feature Extraction for Activity Recognition based on Wavelet Transforms and Adaptive Pooling. In *2019 International Joint Conference on Neural Networks (IJCNN)*, pages 1–8. ISSN: 2161-4393.
- Cola, G., Avvenuti, M., Musso, F., and Vecchio, A. (2016). Gait-based authentication using a wrist-worn device. In *Proceedings of the 13th International Conference on Mobile and Ubiquitous Systems: Computing, Networking and Services, MOBIQUITOUS 2016*, page 208–217, New York, NY, USA. Association for Computing Machinery.
- Gomaa, W., Elbasiony, R., and Ashry, S. (2017). Adl classification based on autocorrelation function of inertial signals. In *2017 16th IEEE International Conference on Machine Learning and Applications (ICMLA)*, pages 833–837.
- Kwapisz, J. R., Weiss, G. M., and Moore, S. A. (2010). Cell phone-based biometric identification. In *2010 Fourth IEEE International Conference on Biometrics: Theory, Applications and Systems (BTAS)*, pages 1–7. ISSN: null.
- Lara, O. D. and Labrador, M. A. (2013). A Survey on Human Activity Recognition using Wearable Sensors. *IEEE Communications Surveys Tutorials*, 15(3):1192–1209.
- Mondol, M. A. S., Emi, I. A., Preum, S. M., and Stankovic, J. A. (2017). Poster Abstract: User Authentication Using Wrist Mounted Inertial Sensors. In *2017 16th ACM/IEEE International Conference on Information Processing in Sensor Networks (IPSN)*, pages 309–310. ISSN: null.
- Murray, M., Drought, A., and Kory, R. (1964). Walking patterns of normal men. *The Journal of bone and joint surgery. American volume*, 46:335–360.
- Ngo, T. T., Makihara, Y., Nagahara, H., Mukaigawa, Y., and Yagi, Y. (2014). The largest inertial sensor-based gait database and performance evaluation of gait-based personal authentication. *Pattern Recognition*, 47(1):228–237.
- Patel, S., Park, H., Bonato, P., Chan, L., and Rodgers, M. (2012). A review of wearable sensors and systems with application in rehabilitation. *Journal of Neuro-Engineering and Rehabilitation*, 9(1):21.
- Shumway, R. H. and Stoffer, D. S. *Time series analysis and its applications : with R examples*. Springer, Cham.
- Tao, S., Zhang, X., Cai, H., Lv, Z., Hu, C., and Xie, H. (2018). Gait based biometric personal authentication by using MEMS inertial sensors. *Journal of Ambient Intelligence and Humanized Computing*, 9(5):1705–1712.